Biologically formed silver nanoparticles and *in vitro* study of their antimicrobial activities on resistant pathogens

Asmaa R. Ali, Haneya A.A. Anani*, Fatma M. Selim

Department of Medical Microbiology and Immunology, Faculty of Medicine for Girls, Al-Azhar University, Cairo, Egypt

ABSTRACT

Background and Objectives: Silver nanoparticles (AgNPs) have been found to have multiple uses as antibacterial, antifungal and anti-biofilm agents because of their biological activities and safety. The present study was aimed to analyze the antimicrobial and anti-biofilm activities as well as the cytotoxic effect of AgNPs against different human pathogens.
Materials and Methods: AgNPs were synthesized using cell free supernatants of *Escherichia coli* (ATCC 25922), *Enterococcus faecalis* (ATCC 19433), *Pseudomonas aeruginosa* (ATCC 27856), *Enterobacter cloacae* (ATCC 13047) and *Penicillium oxalicum* strain, then were analyzed using UV/Vis Spectral Analysis, Transmission electron microscopy (TEM). Scanning Electron Microscope (SEM) and Energy Dispersive-X-ray Spectroscopy (EDX) analysis. Antimicrobial activities of biosynthesized AgNPs were assessed with selected antimicrobial agents against multidrug resistant bacteria and candida. Anti-biofilm and cytotoxicity assays of these biosynthesized AgNPs were also done.
Results: The synthesis of AgNPs were confirmed through observed color change and monitoring UV-Vis spectrum which showed homogeneous (little agglomeration) distribution of silver nanoparticles. TEM and SEM have shown that the particle size ranged from 13 to 34 (nm) with spherical shape and a high signal with EDX analysis. Antibacterial and antifungal efficacy of antibiotics and fluconazole were increased in combination with biosynthesized AgNPs against resistant bacteria and candida. Significant reduction in biofilm formation was found better with *Penicillium oxalicum* AgNPs against biofilm forming bacteria.
Conclusion: *Penicillium oxalicum* has the best effect towards synthesizing AgNPs, for antimicrobial activities against resistant bacteria and candida, in addition to anti-biofilm activities against biofilm forming *Staphylococcus aureus* and *E. coli* and the safest cytotoxicity effect on (MRC-5) cell line.

Keywords: *Penicillium oxalicum*; Sliver nanoparticles; Biofilm; Cytotoxicity

INTRODUCTION

Antimicrobial resistance raises morbidity, mortality, hospital stay length, and healthcare expenses. Antibiotic resistance has been associated to a variety of microbial features, antibiotic using selective pressure, and social and technological changes that facilitate the spread of resistant organisms (1).

Advances in nanotechnology have opened new horizons in nano-medicine, facilitating the synthesis of NPs that are now considered a viable alternative to antibiotics and seem to have high potential to solve the problem of the microbial multidrug resistance (2).

The biological synthesis known as the Green method has been generally considered an alternative to physiochemical methods, due to its cost effectiveness, safety and non-toxicity. Biologically formed silver nanoparticles, are nontoxic for humans (in low

*Corresponding author: Haneya A.A. Anani, Ph.D, Department of Medical Microbiology and Immunology, Faculty of Medicine for Girls, Al-Azhar University, Cairo, Egypt.   Tel: 01019152791   Email: haneyaanani.micro@azhar.edu.eg

concentrations), and are stable inorganic antibacterial agents that have been found to have toxic effect to a wide variety of microorganisms.

The powerful antibacterial and broad-spectrum activity against pathogens seems to be associated with a multifaceted mechanism by which nanoparticles interact with microbes. It seems that antimicrobial activity of AgNPs is rely on monovalent ionic silver, which is released into the microbial cells and inhibits microbial growth by suppressing of respiratory enzymes and electron transport components (3). Furthermore, their particular structure and the multiple modes of interaction with bacterial surfaces may give a specific antibacterial mechanism to be used (4).

In this work, silver nanoparticles were widely used as antibacterial, antifungal, and antibiofilm activities, particularly through biologically generated methods that are safe and reliable.

Aim of the current study was to evaluate of antimicrobial and anti-biofilm activities against different human pathogens as well as cytotoxic activity of silver nanoparticles (AgNPs).

MATERIALS AND METHODS

Reference strains used for silver nanoparticles biosynthesis. In our study we used reference strain to synthesized nanoparticles *Enterococcus faecalis* (ATCC 19433), provided by microbiological resources center (Cairo MIRCEN), Faculty of Agriculture, Ain-Shams University and *Escherichia coli* (ATCC 25922), *P. aeruginosa* (ATCC 27856), *Enterobacter cloacae* (ATCC 13047) kindly supplied from bacteriology laboratory of NAMRU-3. In addition, one isolate of *Penicillium fungus* kindly supplied by Milk and Economy Department, Faculty of Agriculture, Al-Azhar University for which additional purification and identification were done.

Clinical isolates for assessment of antimicrobial activities of silver nanoparticles. Sixty (Forty-one bacterial and nineteen fungal isolates) multidrug resistant isolates were isolated from 166 various clinical samples that were collected from patients admitted to Al Menshawy General Hospital, Egyptian Ministry of Health in the period from January 2018 to September 2019. Bacterial isolates were inoculated onto nutrient agar, MacConkey's agar and blood agar plates then incubated at 37°C to isolate pure colonies.

Suspected pure colonies were identified on the basis of conventional identification such as sugar fermentation, indole test, lysine iron agar and MIO test, citrate test and coagulase test. Selected candida isolates were *Candida albicans* (6), *Candida glabrata* (6), *Candida tropicalis* (3) and *Candida krusei* (4). All candida isolates were purified and identified in a Sabouraud's dextrose agar (SDA) medium and cornmeal agar containing Tween 80 with production of chlamydospores and germ tube test (5). In order to screen for carbapenems-resistant isolates, methicillin resistant *Staphylococcus aureus* (MRSA) isolates and fluconazole resistant candida (FRC) isolates were tested according to Kirby-Bauer disc diffusion test. The findings have been interpreted according to methods of CLSI guidelines (6, 7). Pure isolates were stored for various application of silver nanoparticles until use.

Ethical approval. The used protocol was approved by the Committee of Ethics of the Faculty of Medicine for Girls, Al-Azhar University. The approval number (201911259) was obtained by author. An informed written consent was received from patients. The present work was conducted in accordance with the Declaration of Helsinki.

Bacterial biosynthesis of silver nanoparticles. All bacterial reference strains were inoculated onto nutrient agar, MacConkey agar and blood agar plates, bile esculin agar and incubated at 37°C overnight to isolate pure colonies. Suspected pure colonies were subjected to Gram stain and biochemical reactions were tested according to Cheesbrough, (2006) (5).

Preparation of silver nitrate solution (1Mm). 1.6 Gram of silver nitrate (AgNO$_3$) was dissolved in one liter of sterile double distilled water. The solution was held in dark condition at 4°C for not more than 2 weeks.

Production of cell supernatant from different bacteria. Silver nanoparticles synthesis was carried out using a method modified from Saeb et al. (2014) (8). In which nanoparticles preparation was performed as follows: sterile nutrient broth was inoculated with different pure bacterial isolates. The culture flasks were incubated at 37°C. After incubation time, the culture flasks were centrifuged at 6.000 rpm for 10 minutes then supernatant was filtered and used for silver nanoparticle synthesis. Erlenmeyer flasks

containing 90 ml of different bacterial supernatants were mixed with 10 ml $AgNO_3$. The flasks were incubated at 37°C with shaking in dark condition. The production of silver nanoparticles was confirmed by monitoring the observed color change from yellow to light or dark brown. Newly formed silver nanoparticles were prepared and stored at 4°C in dark condition. Two negative control flasks, one contained the supernatant of bacterial broth culture only and the other contained 1 mM $AgNO_3$ solution only were included in each run to check the purity and quality of the reagents as shown in Fig. 1.

Fig. 1. (A) Color change from yellow to dark brown of aqueous solution filtrate of *Penicillium fungus* after treatmentwith $AgNO^3$. (B) Shows a flask of fungal biomass in aqueous solution.

Mycosynthesis of sliver nanoparticles. Mycosynthesis was done by a method modified from that of Ottoni et al. (9). From stock cultures grown in SDA, a small piece from the peripheral area of the agar was cut by a sterile blade and transferred by sterile forceps onto the center of a new SDA medium, then incubated for 7 days at room temperature in a dark area. Biomasses of fungus were obtained by inoculating two culture disks (10 mm diameter) of each isolate in 100 ml of SD broth. The cultures flasks were incubated for 4 days with shaking at 30°C. Biomass was obtained by filtration and washed several times. Fungal mycelia were incubated in 100 ml of sterile distilled water in shaker incubator at 30°C for 3 days. The supernatant was purified into 0.2 μm millipore filter and used as a source of sliver nanoparticles. 90 ml of the previous supernatant was then added to 10 ml of silver nitrate ($AgNO_3$) solution (1 mM), followed by incubation for 3 days in the dark condition. Production of silver nanoparticles was confirmed through monitoring the change of color from yellow to dark brown. Two control flasks, one contained the supernatant of fungal broth culture only and the other contained 1 mM $AgNO_3$ solution only were incubated in each run to check for the quality of the reagents and contamination.

Silver nanoparticles synthesis by chemical reduction method. 50 ml of 0.001 M $AgNO_3$, in Erlenmeyer flask was heated to boil in magnetic stirrer. 10 ml of 1% trisodium citrate was added very slowly to obtain a good distribution. When the color changed to yellow, the flask was withdrawn from the heater. The solution was stored at 4°C in the dark area (10).

Characterization of silver nanoparticles. The characterization of silver nanoparticles was carried out at TEM and SEM Units, Mycology Regional Center, Al-Azhar University.

Ultraviolet UV/vis spectral analysis. AgNPs solution wavelength was recorded using a UV/vis spectrophotometer form 300-700 nm operated at a resolution of 1 nm. Absorbance was graphed and compared to the published data (11) (Fig. 2).
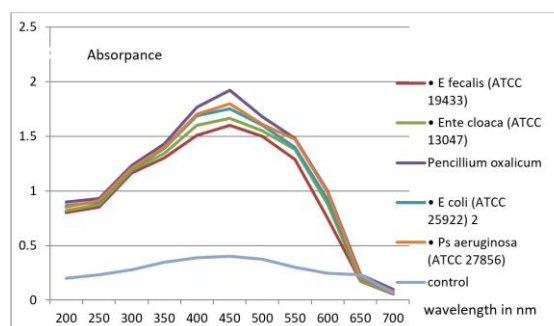

Fig. 2. UV-Vis absorption spectrum of silver nanoparticles synthesized by different microorganism.

Transmission Electron Microscopy (TEM). The size and morphology of the synthesized nanoparticles were reported by using carbon coated grids (PELCO 50 USA), then examined by TEM (JEOL 60-150) (12) (Fig. 3).

Scanning electron microscope (SEM). The morphology and size of the synthesized NPs were studied by SEM using JEOL JSM 5500 LV scanning electron microscope. Preparation of slides by using a typical SEM coater, the powder was pressed to the carbon tape with a fine layer (thin film of gold) and then ana-
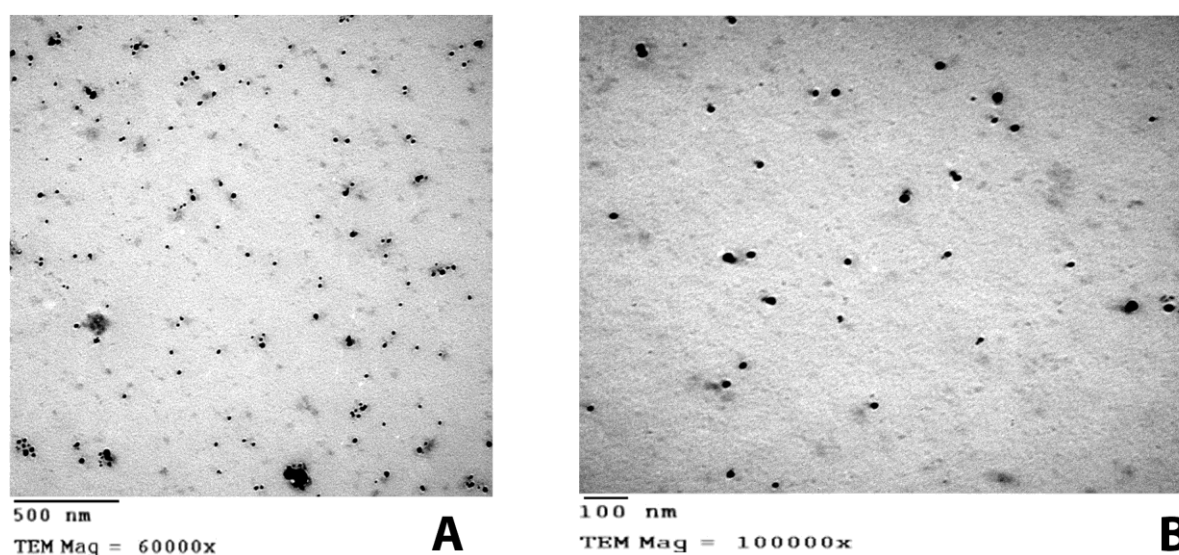
Fig. 3. Transmission electron image of AgNPs produced by (A) *P. aeruginosa* isolate (spherical shape with particle size ranged from 13 to 34 nanometer (nm), without significant agglomeration at magnification power 60000 X. (B): *Enterococcus faecalis* isolate (spherical and hexagonal in shape and the particle size ranged from 34 to 55 at magnification power 100000 X. They were found to be either aggregated or as a single granule at certain locations.

lyzed by SEM. The microscope operated at an accelerated voltage at 5-10 KV at different magnifications, low vacuum, a spot size 4 and working distances 1-10 mm (12) (Fig. 4).

Energy Dispersive-X-ray spectroscopy analysis (EDX). The elemental analysis of the single particle was carried out using EDX attached with the SEM at 10KV (13) (Fig. 5).

Molecular identification of penicillium isolate. The penicillium isolate was further submitted to molecular identification by 18S rDNA sequencing-based method to ascertain its taxonomic position.

DNA extraction. DNA extraction of the Penicillium isolate was done by the QIAGEN® Genomic-tip - (EN) as directed by the manufacturer (14). PCR assay was conducted using thermal cycler based on amplification of 18S rDNA. The primers (Invitrogen, Germany) were selected from published sequences (15). The sequences of primers used for amplification of 18S rDNA gene were

Forward. 5` GCA TCG ATG AAG AAC GCA GC 3`
Reverse. 5` TCC TCC GCT TAT TGA TAT GC 3`

Amplification. The total reaction volume was 50 ml containing 15 ml nuclease free water, 1 ml (20 Pi-

comole) of each primer (Invitrogen, Germany), 25 ml (MyTaq Red Mix), (Qiagen, Germany Genomic-tip - (EN) and 8 ml of the extracted DNA. Amplification conditions included an initial denaturation stage at 94°C for 5 minutes followed by 35 cycles. Each cycle consists of; denaturation at 94°C for 1 minute, annealing at 56°C for 1 minute, an extension at 72°C for 1minute and followed by a final extension at 72°C for 7 minutes. The amplified products were separated by 2% agarose gel and were further subjected to sequencing using DNA sequencer (Roche-454GX-FLX Switzerland). The sequence data were subjected to BLAST analysis and the result revealed its maximum identity to different penicillium species and most likely to *Penicillium oxalicum* (99.9%). The 18S rDNA sequence of the isolate was sent to NCBI by gene bank accession number MT533785.

Antimicrobial study of the synthesized silver nanoparticles. 100 ul (100 µg/ml) of synthesized AgNPs were used for their antimicrobial effect by the agar well diffusion test against different kinds of multidrug resistant microorganisms (16).

Antibacterial activity of AgNPs alone and combined AgNPs-amoxicillin on MRSA isolates. Mixture preparation of both concentration of amoxicillin (25 µg/ml) and AgNPs (100 µg/ml), then vortexed
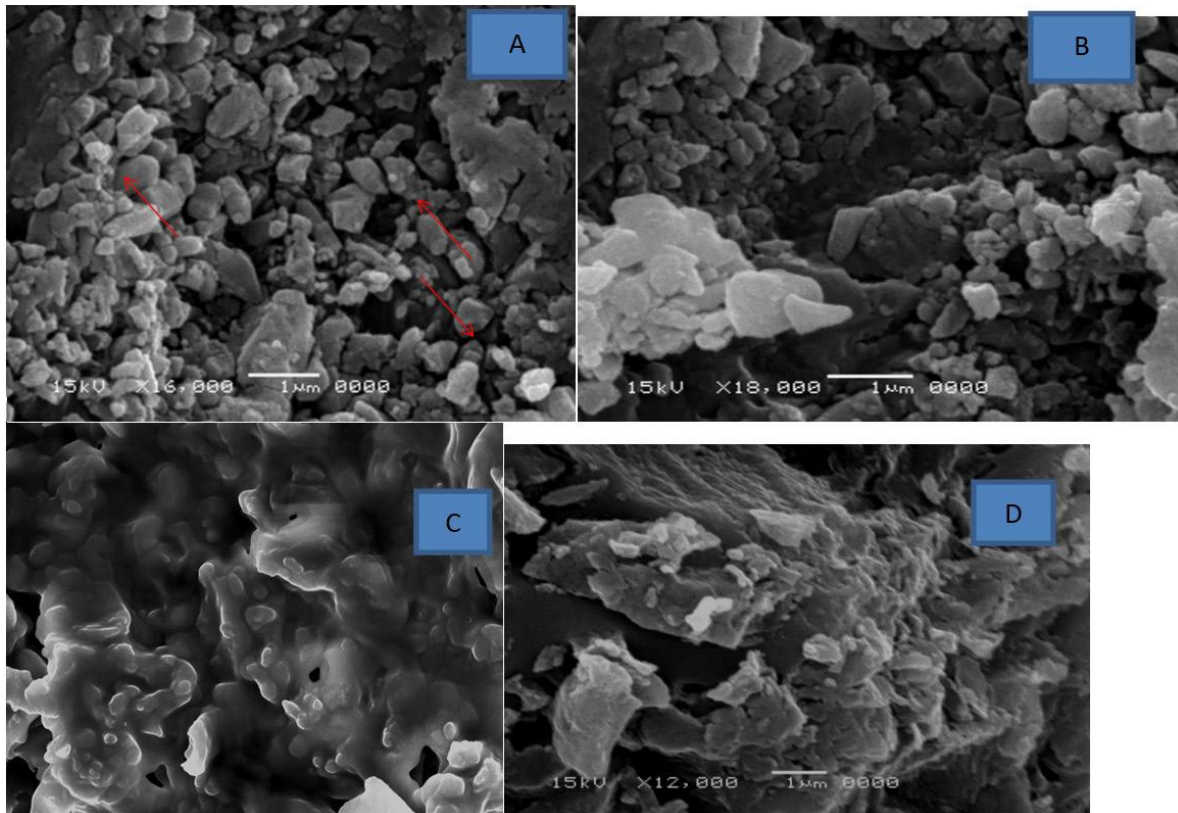
Fig. 4. SEM image showed reduction of silver nitrates particles into oval and triangular nanoparticles by (A) *Penicillium fungus* at magnification power 16,000 X, (B) *Enterobacter cloacae* with particle size ranging from 7-55 nm at magnification power 18,000 X (C) and (D) *Enterococcus faecalisat* magnification 12,000 X. Most of the NPs were aggregated in the form of clusters, and only few of them were scattered. SEM absorption of the products was recorded as synthesis of nanoparticles spherical and triangular in structure of about 7-55 nm in diameter. Most of the NPs were aggregated in the form of clusters, and only few of them were scattered.
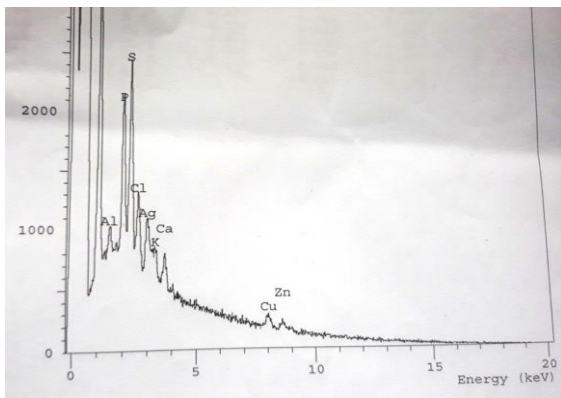

Fig. 5. EDX spectrum of biosynthesized silver nanoparticles. The EDX spectrum was recorded in the spot-profile mode, strong signals from the sodium (Na) sulphur, (S), phosphorus (P) and silver (Ag) atom were observed while medium signals from Cu and weaker signals from other atoms. The optical absorption peak of AgNPs was observed at 3 keV which is atypical absorption of metallic AgNPs.

for 15 minutes. The antibacterial activity of AgNPs alone and in combination with amoxicillin (25 µg/ml) on 16 methicillin resistance *Staphylococcus aureus* (MRSA) isolates was investigated by agar well diffusion test. The bacterial suspension was adjusted to 10^8 CFU \ml. The zones of inhibition were measured in triplicate and the mean values ± SD were recorded (17).

Antibacterial activity of AgNPs on carbapenems resistance Enterobacteriacea (CRE) alone and combined AgNPs-gentamicin. The antibacterial activity of AgNPs alone and mixed with gentamicin (30 µg/ml) on 22 carbapenems resistance Enterobacteriacea (CRE) isolates (16 *K. pneumoniae* and 6 *E. coli*) were investigated by agar well diffusion test. The zones of inhibition were determined in triplicate and the mean values ± SD were recorded (17). The increase in the fold area of different pathogens for antibiotics and antibiotics combined with silver nanopar-

ticle solution can be calculated by fold increase (%) = [(b−a)/a] ×100 where "a" refer to the zones of inhibition for antibiotic alone and "b" the zones of inhibition for antibiotic with silver nanoparticles (18) (Figs. 6 and 7).

Antifungal activity of AgNPs on fluconazole-resistant candida isolates alone (FRC) and combined AgNPs-fluconazole. The antifungal activity of *Penicillium oxalicum* biosynthesized AgNPs alone and mixed with fluconazole (10 μg/ml) was investigated on 15 FRC isolates by agar well diffusion test (18), which the fungal suspension was adjusted to 10^5 CFU \ml. Four wells (6 mm diameter) were punched in SDA plates using sterile corkborer after inoculation with fungal culture. The zones of inhibition were determined in triplicate and the mean values ± SD were recorded (19).

Anti-biofilm activity of AgNPs using crystal violet assay. Biofilm inhibition carried out in 96 well plates adopting modified method of biofilm inhibition spectrophotometric assay (20). To adjust the working solution to be 1024 ug/ml. Dilution of 1mg to 7.8 μg/ml of AgNPs samples, 8 tubes were prepared with 1000 μg/ml, 500 μg/ml, 250 μg/ml, 125 μg/ml, 62.5 μg/ml, 31.2 μg/ml, 15.6 μg/ml and 7.8 μg/ml respec-

tively. 100 ml of cell suspension of biofilm forming *E. coli* and *S. aureus* were added into 96 well titer plate. 100 ml of previous concentration of different AgNPs were added in each well of 96-well plate in duplicates and the plate was incubated at 37°C for 24 hours. After the incubation, the liquid suspension was
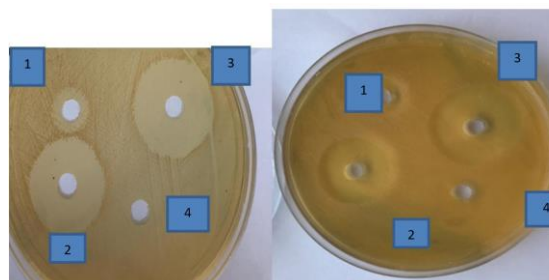

Fig. 7. Antimicrobial activity of silver nanoparticles against (A) carbapenem-resistant *E. coli* (B) MRSA. AgNPs had respectable inhibition zone against CR *E. coli* and MRSA strain. (A) (1) The zone of inhibition produced by gentamycin 14.50 mm, (2) The zone of inhibition of AgNPs alone 29.4 mm (3) combined AgNPs with gentamycin 32 mm (4) control 0 mm . While the AgNPs zone of inhibition against (B) MRSA (1) AgNPs alone 21.2 mm, (2) amoxicillin 14.3 mm (3) combined AgNPs with amoxicillin 23.4 mm, (4) control 0 mm. Combined AgNPs with antibiotics have greater antibacterial activity compared to antibiotics alone.
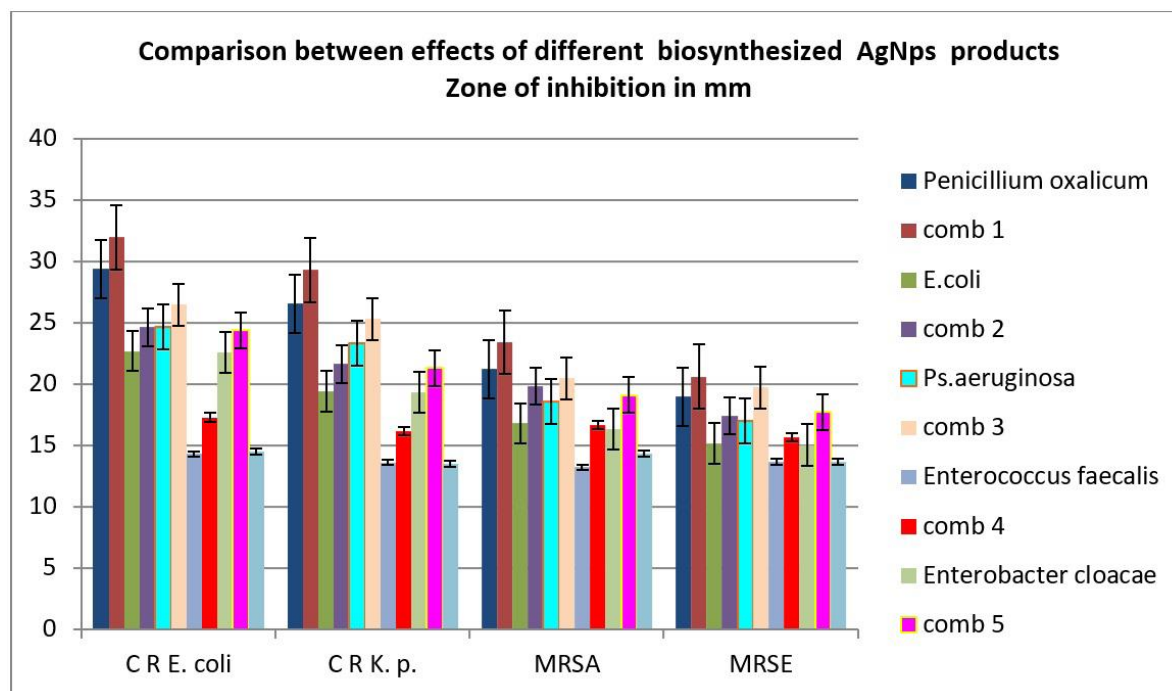

Fig. 6. Synergistic antibacterial effect between all biosynthesized AgNps and antibiotics against multidrug resistance bacteria

discarded and 100 ml of 1% w/v aqueous solution of crystal violet was added for staining at room temperature for 30 minutes. The staining dye was discarded and the plate was washed 3 times with 300 ml of distilled water. 95% ethanol was added and incubated for 15 minutes. The O.D. absorbance was read at 570 nm using a microplate reader (TECAN, Inc.) within 30 min after gentle shaking (20) (Fig. 8).

Cytotoxicity viability assay. The cells were seeded in 96-well plate at a cell concentration of 1×10^4 cells per well in 100 ml of growth medium. Fresh medium containing different concentrations of the biosynthesized AgNPs was added after 24 hours of seeding. Serial two-fold dilutions of the AgNPs were added to confluent cell monolayers dispensed into 96-well, microtiter plates. The microtiter plates were incubated at 37°C in a humidified incubator with 5% CO_2 for a period of 24 h. Three wells were used for each concentration of the AgNPs. Control cells were incubated without AgNPs and with or without DMSO. The little percentage of DMSO present in the wells (maximal 0.1%) was not found to affect the experiment. Then viability of cells was measured by a colorimetric method. The media was discarded and 100 ml of fresh culture RPMI 1640 medium without phenol red was added then 10 ml of the 12 mM MTT stock solution

(5 mg of MTT in 1 ml of PBS) was added to each well including the untreated controls. The plates were then incubated at 37°C and 5% CO_2 for 4 hours. An 85 ml aliquot of the media was removed from the wells, and 50 ml of DMSO was added to each well and mixed thoroughly and incubated at 37°C for 10 minutes (21) (Fig. 9).

Calculation of results. The O.D. absorbance was read at 590 nm using a microplate reader (SunRise, TECAN, Inc, USA) within 30 minutes, then determine the number of viable cells and the percentage of viability was calculated as [(OD t /OD c)]×100% where OD t is the mean optical density of wells treated with the AgNPs and ODc is the mean optical density of untreated cells.

The standard curve of each cell line was plotted as the relation between surviving cells after treatment with AgNPs and AgNPs concentration.

The cytotoxic concentration (CC50), the concentration required to cause toxic effects in 50% of intact cells, was estimated from graphic plots of the dose response curve for each conc. using Graph-pad Prism software (San Diego, CA. USA) (22).

Analyzing data. The data was analyzed using Statistical Program for Social Science (SPSS) version

Fig. 8. Anti-biofilm activity of different biosynthesized AgNps on biofilm forming *Staphylococcus aureus*. The MBIC value is defined as the lowest concentration to inhibit 100% of bacterial biofilm under the assayed conditions. The MBIC of *Penicillium oxalicum* and *P. aeruginosa* AgNps on biofilm forming *E. coli* were 31.25 and 125 ug/ml respectively. However The MBIC of *Penicillium oxalicum* and *P. aeruginosa*. AgNps on biofilm forming *Staphylococcus aureus* were 62.5 and 125 ug/ml respectively.

Fig. 9. Evaluation of cytotoxicity of different biosynthesized AgNps products against MRC-5 cell line. Inhibitory cytotoxic activity of AgNps against normal human lung fibroblast cell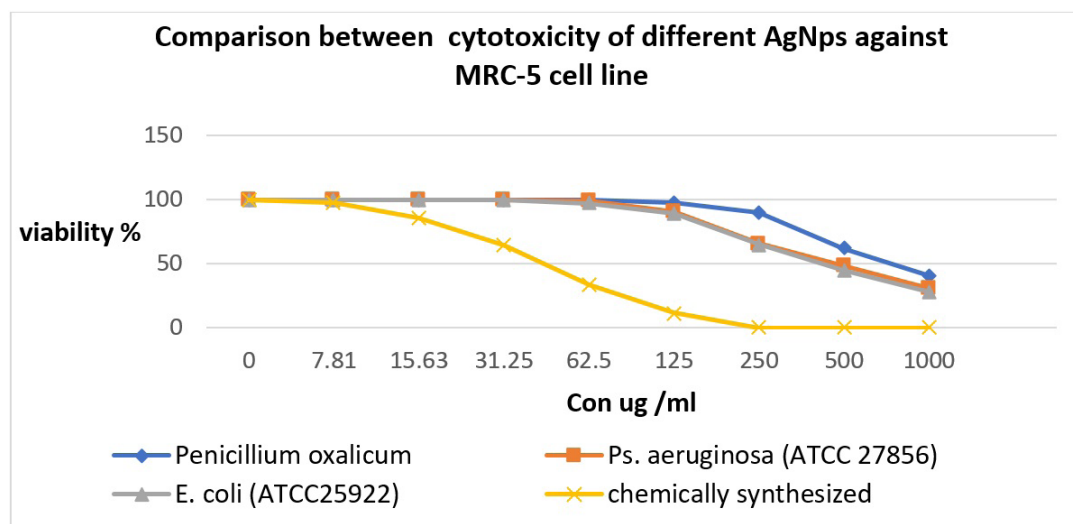s was detected using MTT assay with cytotoxic concentration (CC_{50}) required to cause toxic effects in 50% of intact cells. Chemically synthesized AgNps were the most toxic against MRC-5 cell line. (CC_{50} = 31.5 ug/ml) and *Penicillium fabricated* AgNps were the least toxic against the same cell line (CC_{50} =500 ug/ml)

20. Data. The mean± standard deviation (SD) was expressed as quantitative result. Independent t-test of significance was used when comparing between two means. ANOVA test was used to compare between different times in the same group in quantitative data. Chi-square ($X2$) test of significance was used in order to compare proportions between two qualitative parameters.

RESULTS

Silver nanoparticles biosynthesis. Formation of silver nanoparticles were observed after 24 hours by changing the color from light yellow to dark brown as shown in Fig. 1 (1).

The characterization of silver nanoparticles was done by using UV-Vis spectrum TEM, SEM and EDX analysis. UV-Visible absorption spectrum of silver nanoparticles synthesized by different strain and chemical reduction showed *Penicillium oxalicum* isolate showed the best results with the highest optical density. Descriptive data of synthesized nanoparticles using Transmission Electron Microscopy revealed that in *Penicillium oxalicum* have spherical and triangular in shape and the size ranged from 8 to 15 nm with no observed agglomeration. In *Pseudomonas aeruginosa* isolates have spherical shape and the size ranged

from 13 to 34 nm, without significant agglomeration while in *Enterococcus faecalis* isolates have spherical and hexagonal in shape and the size ranged from 34 to 55 nm. They were found to be either aggregated or as a single granules at certain locations analysis. In SEM the absorption of the products was recorded as synthesis of nanoparticles spherical and triangular in structure of about 7-55 nm in diameter. Most of the NPs were aggregated in the form of clusters, and only few of them were scattered. In EDX analysis, the presence of elemental silver indicated the reduction of silver ion in the reaction mixture by bacterial cell free filtrate mixtures into silver metal.

Antibacterial study of silver nanoparticles. Antimicrobial activity of AgNPs against 60 resistant isolates (41 bacterial and 19 candida isolates) were identified by antimicrobial susceptibility as (13 MRSA isolates, 6 MRSE isolates, 16 carabapenems- resistant *Klebsiella pneumoniae*, 6 *E. coli*) were evaluated using agar well diffusion test. Also antifungal study was done on 19 fluconazole resistant candida as 6 (*Candida albicans*), 6 (*Candida glabrata*), 3 (*Candida tropicalis*) and 4 (*Candida krusei*) (Tables 1, 2 and 3).

DISCUSSION

The production of nanoparticles with antibacterial

Table 1. Efficacy of single antibiotic and mixed sliver nanoparticles (AgNps) with antibiotic on carbapenem-resistant *E. coli* and *K. pneumoniae* by agar well diffusion in mm

		Escherichia coli (ATCC 25922) Mean + SD	*Enterococcus faecalis* (ATCC 19433) Zone of inhibition (mm) ± SD	*Enterobacter cloacae* (ATCC 13047) Zone of inhibi-tion (mm) ± SD	*P. aeruginosa* (ATCC 27856) Zone of inhibi-tion (mm) + SD	*Penicillium oxalicum* Zone of inhibi-tion (mm) ± SD
E. coli						
AgNps		22.72 ± 0.73	14.33 ± 1.03	22.60 ± 2.88	24.67 + 1.75	29.42 + 2.01
AgNps + Gentamycin		24.65 ± 1.56	17.3 ± 1.48	24.43 ± 2.56	26.50 + 1.05	32.00 + 1.41
Gentamycin		14.50 + 1.05				
ANOVA	No.	128.520	11.500	31.516	142.826	214.188
	P value	<0.001**	<0.001**	<0.001**	<0.001**	<0.001**
Fold increase %		70%	19.3%	68.5%	82.7%	120%
K. pneumoniae						
AgNps		19.44 + 1.26	13.63 ± 1.09	19.34 + 1.44	23.34 + 1.40	26.56 + 1.72
AgNps + Gentamycin		21.65 ± 1.56	16.19 ± 1.33	21.31 + 1.05	25.31 + 1.25	29.34 + 1.78
Gentamycin		13.50 + 1.10				
ANOVA test		163.007	26.507	180.539	406.324	467.994
		<0.001**	<0.001**	<0.001**	<0.001**	<0.001**
Fold increase %		60.4%	19.92%	57.8%	87.5%	117%

ANOVA test was used for comparison between individual antibiotic and combined sliver nanoparticles (AgNps) with antibiotic on carbapenem-resistant *E. coli* (<0.001** Highly significant)

properties has received attention among researchers. The growing threat from resistant organisms calls for concerted action to avoid the dissemination of new resistant strains and the spread of existing ones (23).

We screened four different reference bacterial strains and one filamentous fungus for the potential reduction the silver ions to AgNPs. Based on our observations, the selected strain was capable of extracellular biosynthesis of AgNPs by reducing silver nitrate and the change of color was observed from pale yellow to brown.

The UV-Vis absorption spectra of all bacterial cell free suspensions were measured and a high peak in the visible region at 415 nm was obtained to confirm the presence of AgNPs. Our results corroborated with other study (24), they reported that an observation of a wide surface plasmon peak in the ranged from 415 to 430 nm is characteristic of silver nanoparticles due to its surface plasmon resonance which represents the collective excitation of conduction electron in metal. The absorption spectrum of the silver nanoparticles is shown to indicate the formation of the nanoparticles where the presence of a plasmon absorption band at ~ 415-430 nm is characteristic of silver nanoparticles. The surface of a metal is like plasma, having free electrons in the conduction band and positively charged nuclei. Earlier studies have shown that AgNPs synthesized using different microbes such as *Pseudomonas stutzeri, Bacillus megaterium, K. pneumoniae*, and *Bacillus licheniformis* have greater particle sizes of 200 nm, 80-98.56 nm, 28.2-122 nm, and 50 nm, respectively. Our finding that the particle size of *Penicillium oxalicum* AgNps varied was (8-15 nm). The particles were round and triangular, with little aggregation. These findings are in line with results of Ansari et al. who discovered that *Deinococcus radiodurans* biosynthesized AgNPs have size 16.82 nm (25). The fungus *Penicillium* makes a suitable option for the production of metallic nanoparticles since it secretes large amount of proteins, thereby increasing efficacy and making them easy to use in the laboratory (23).

The AgNPs were found to be well distributed in SEM, with a triangular and spherical form and partial aggregation. The aggregation observed by (26), in their study on the production of AgNPs using soil-isolated penicillium strains. Our findings corroborated those of Magudapathy et al. who found that the biosynthesized AgNPs by cell free supernatant of *Lactobacillus casei* and *Lactobacillus fermentum*

Table 2. Efficacy of single antibiotic and mixed sliver nanoparticles (AgNps) with antibiotic on Methicillin resistant *Staphylococcus aureus* (MRSA) and Methicillin resistant *Staphylococcus epidermidis* (MRSE) by agar well diffusion through measuring the zone of growth inhibition in mm

		E. coli (ATCC 25922) Zone of inhibition (mm) + SD	*Enterococcus faecalis* (ATCC 19433) Zone of inhibition (mm) + SD	*Enterobacter cloacae* (ATCC 13047) Zone of inhibition (mm) + SD	*P. aeruginosa* (ATCC 27856) Zone of inhibition (mm) + SD	*Penicillium oxalicum* Zone of inhibition (mm) + SD
MRSA						
AgNps		16.82 ± 0.72	13.25 + 1.00	16.35 ± 1.44	18.63 + 1.36	21.25 + 1.69
AgNps + Amoxicillin		19.83 ± 1.13	16.67 ± 1.52	19.12 ± 1.65	20.50 + 1.03	23.44 + 1.55
Amoxicillin		14.38 + 1.20				
ANOVA	No.	89.499	24.927	35.461	88.171	130.10
	P value	<0.001**	<0.001**	<0.001**	<0.001**	<0.001**
Fold increase %		37.9%	15.9%	33.6%	42.6%	63%
MRSE						
AgNps		15.17 + 1.04	13.67 + 0.58	15.05 + 1.35	17.00 + 1.00	19.00 + 1.00
AgNps + Amoxicillin		17.44 + 1.00	15.66 ± 1.4	17.75 + 1.05	19.75 + 1.05	20.61+ 0.58
Amoxicillin		13.67 + 1.53				
ANOVA test		F =14.663	F =5.124	F = 14.722	F = 37.551	F= 64.584
		<0.001**	0.020*	<0.001**	<0.001**	<0.001**
Fold increase %		27.6%	14.6%	29.8%	44.5%	50.8%

ANOVA test was used to compare between different groups (>0.05 Non significant <0.05* significant <0.001** High significant). Synergistic efficacy of silver nanoparticles was observed with gentamycin against Carbapenem- resistant *Enterobacteriace* and with amoxicillin against MRSA. The best activity was observed with *Penicillium oxalicum* strain biosynthesized AgNPs followed by *P. aeruginosa* (ATCC 27856). Carbapenem- resistant *E. coli* was more susceptible than *K. pneumoniae* and MRSA was more susceptible than MRSE

were spherical with a size of around 10.0 nm and aggregated, possibly due to the drying process (27).

The combination of (SEM) with (EDX) can be used for examination of silver powder morphology and chemical composition analysis. The EDX analysis of silver nanoparticles revealed a high signal at 3 keV in the silver region and thus confirmed the presence of silver nanoparticles in the prepared sample suggested a reduction of Ag^+ ions to elemental silver. The percentage of elemental constituents for silver nanoparticles in *Penicillium oxalicum* (mean ± SD 19.57 - 25.2% ± 0.372%) while in chemically synthesized particles (mean ± SD 25.765 - 33.538 ± 2.77%) Our findings are comparable to those of another study, which found that metallic silver nanoparticles have an optical absorption peak of around 3 keV due to surface plasmon resonance (28).

The synergistic effect of AgNPs has a wide variety of activity against different types of bacteria (10). In the present work, the AgNPs produced by *Penicillium oxalicum* strains were found to be active against *E. coli, K. pneumoniae, S. aureus, S. epidermidis.* By using agar well diffusion, the antibacterial activities were assayed against 6 carbapenems-resistant *E. coli* and 13 MRSA. The best activity was observed with *Penicillium oxalicum* (29.42, 20.25 and 25 mm respectively) followed by biosynthesized AgNPs from *P. aeruginosa* (ATCC 27856) (27.84, 18.63 + 1.36 and 23.57 mm) compared to other strains (*Escherichia coli* ATCC 25922) AgNPs (26.73, 18.87 and 22.65 mm respectively), (*Enterobacter cloacae* ATCC 13047) AgNPs (25.6, 17.35 and 20.43 mm respectively) and (*Enterococcus fecalis* AgNPs ATCC 19433) (23.22, 16.1 and 18.3 mm respectively). Wisam et al. (2018) found that at a concentration of 200 ug/ml, the diameter of the inhibition zones of Zingiber officinal plant extract biosynthesized AgNPs against bacterial strains such as *Bacillus subtilis* (31 mm) and *E. coli* (30 mm) was 31 mm (29).

The antibacterial effects of AgNPs on Gram positive and Gram negative organisms were explored in our study, and they demonstrated stronger antibacte-

Table 3. Antifungal activities of all biosynthesized AgNps. against different fluconazole resistant candida isolates

	E. coli (ATCC 25922) Zone of inhibition (mm) + SD	E. faecalis (ATCC 19433) Zone of inhibition SD	Enterobacter cloacae (ATCC 13047) Zone of inhibition (mm) + (mm) + SD	P. aeruginosa (ATCC 27856) Zone of inhibition (mm) + SD	Penicillium oxalicum Zone of inhibition (mm) + SD
Candida albicans					
AgNps	20.65 ± 1.74	15.33 +1.53	20.23 ± 2.88	22.00 + 1.00	25.00 + 1.00
AgNps + Fluconazole	22.58 ± 1.46	18.07 ± 1.12	22.42 ± 2.64	24.33 ± 1.53	27.67 + 1.53
Fluconazole		11.33 + 1.15			
ANOVA test	100.506	42.052	37.439	185.451	296.560
	<0.001**	<0.001**	<0.001**	<0.001**	<0.001**
Fold increase %	99.3%	59.5%	97.9%	114.7%	144%
Candida glabrata					
AgNps	18.12 + 0.62	14.67 + 0.82	18.23 ± 0.92	20.42 + 0.92	23.50 + 1.33
AgNps+ fluconazole	21.50 + 0.55	17.07 ± 1.32	20.50 ± 1.04	23.50 + 1.05	25.50 + 1.05
Fluconazole		10.83+ 1.17			
ANOVA	260.362	47.131	139.606	236.889	275.354
	<0.001**	<0.001**	<0.001**	<0.001**	<0.001**
Fold increase %	98.5%	57.6%	89.3%	117%	135.4
C. krusei					
AgNps	15.00 + 0.92	10.55 + 0.96	15.63 ± 042	15.75 + 0.96	18.25 + 0.96
AgNps+ fluconazole	17.27 + 1.53	12.67 + 0.58	17.33 ± 0.84	18.25 + 0.50	21.05 + 0.58
fluconazole		9.75 + 1.71			
ANOVA	29.213	6.533	49.878	66.655	99.366
	<0.001**	0.018	<0.001**	<0.001**	<0.001**
Fold increase %	77%	29.9%	77.7%	87.2%	115.9%

Synergistic efficacy of silver nanoparticles was observed with fluconazole against different types of candida. The best activity was observed with *Penicillium oxalicum* strain biosynthesized AgNPs. *Candida albicans* was more susceptible than the other types

rial activity against (CR *E. coli*) than MRSA. Our results are similar to Nanda et al. who found that higher antibacterial activity on Gram-negative (*E. coli* and *Salmonella typhi*) than Gram-positive (*S. aureus* and *S. epidermidis*) bacteria (30). In contrast Long-hi et al. who found that the Gram-positive (MRSA and MRSE) were more susceptible to AgNPs than Gram-negative (*Salmonella typhi* and *K. pneumoniae*) bacteria (31). This seems to be due to variations in the membrane structure and the composition of the cell wall, thereby influencing access of the AgNPs.

Synergistic efficacy of silver nanoparticles with various antibiotics was observed on selected pathogens. The synergistic effect silver nanoparticles with gentamicin against Gram-negative bacteria is higher than that of amoxicillin against Gram-positive bacteria. It indicated that the combination of antibiotics and nanoparticles could improve the effectiveness of

antibiotic against resistant pathogens. Our results are similar to those of, they found that increasing efficacies of antibiotics such as vancomycin, gentamycin, streptomycin, ampicillin, and kanamycin when used in conjunction with AgNPs against *P. aeruginosa, S. aureus,* and *E. coli.*

The antifungal effect of AgNPs against fluconazole resistant strain of candida isolates was investigated using agar well diffusion method. The synergistic effect was observed when AgNPs and FLC were mixed against fluconazole resistant (FR) *Candida albicans* isolates. Our results are agreed with Jalal et al. who observed that the decrease of FLC MIC of FLC-resistant *Candida albicans* when combined to AgNPs (32). Masurkar et al. also reported significant reductions of bacterial growth at concentration (500 ug/ml) of silver nanoparticles (33). This can be explained by the AgNPs can change the permeability

of the cell membrane, we can hypothesize that they may promote the entry of FLC, which interferes with ergosterol biosynthesis.

Synergistic antifungal effect was obtained by combination of different biosynthesized AgNPs with fluconazole on candida isolates .However, the best antifungal effects of *Penicillium oxalicum* biosynthesized AgNPs were better on *Candida albicans* than on other candida species.

The minimal biofilm inhibitory concentration (MBIC) of *Penicillium oxalicum* and *P. aeruginosa* (ATCC 27856) AgNPs on biofilm forming *S. aureus* were 62.5 and 125 ug/ml and on biofilm forming *E. coli* were 31.25 and 125 ug/ml respectively. Our finding is similar to Chaudhari et al. (2012) (34) who investigate the anti-biofilm activity of AgNPs (51 nm) synthesized from *Bacillus megaterium* at a concentration as low as 50 μg/ml and recorded that AgNPs had improved quorum quenching activity against *S. aureus* biofilm and prevention of biofilm formation. They concluded that AgNPs could be active in the prevention of biofilm formation. Similar finding was observed with Kuldeep et al. (2014) (35) who investigated antibiofilm activities of AgNPs *P. aeruginosa, S. aureus* and *C. albicans.* More than 90% biofilm inhibition was observed at 250 ug/mL concentrations and 85% of the biofilm inhibition was observed at 125 ug/mL.

In addition, Kalishwaralal et al. (36) reported that the antibacterial effect of AgNPs on *P. aeruginosa* and *S. epidermidis*, and their effect on biofilm formation at a concentration of 100 μM and the AgNPs inhibit the biofilm formation with 95% and 98%.

Chávez-Andrade et al. (37) revealed that silver nanoparticles had antibacterial and anti-biofilm capabilities against *E. faecalis, Candida albicans*, and *Pseudomonas aeruginosa*, and may be a viable alternative for root canal system disinfection.

Ansari et al. (2015) (26) detect the production of biofilm by extended spectrum β-lactamase isolates of *E. coli* and *Klebsiella pneumoniae*, (MRSA) and methicillin resistant *S. epidermidis* (MRSE) and also studied by using confocal laser scanning microscopy techniques which offer concrete evidence of the ability of 50 μg/ml AgNPs to block bacterial growth and to prevent the glycocalyx formation. An interesting evolution of using nanoparticles toward biofilm forming *P. aeruginosa* is represented by (38) using 100 mg/ml silver-coated magnetic nanoparticles, in fact, design of multimodal nanoparticles comprising

a magnetic core and a silver ring showed promising results.

Our result agreed with Yen et al. who studied the interactions of AgNPs with *P. putida* biofilms and demonstrated that the biofilms are impacted by the treatment with AgNPs at 125 ug/ml (39). The nanoparticles analyzed in their study were of quite large dimensions over 60 nm.

In the present work, the cell viability and metabolic activity were demonstrated using MTT assay by exposing the normal human fibroblast cell line (MRC-5) cells to AgNPs at concentration ranged from 0 μg - 1000 μg for 24 hours. The findings of the MTT assay revealed a dose-dependent decrease in percent viability of the cells (cytotoxicity on MRC-5). The CC50 of *Penicillium oxalicum* biosynthesized AgNPs was in the range of 500 μg/mL, which is much higher than that of chemically synthesized AgNPs 31.5 ug/ml and higher than that of the effective antimicrobial doses. Our results similar to who studied the macrophages treated with AgNPs at a concentration of 10 μg ml. AgNPs used were safe on this type of cell at that concentration (40).

We also agreed with Moteriya et al. who tested the *in vitro* cytotoxicity of Caesalpinia Pulcherrima biosynthesized AgNPs on HeLa cell line using different concentrations (41). The cytotoxic effect on HeLa cell line was increased with an increased concentration of AgNPs. The cell viability was 100% at a lower concentration of AgNPs and 42% of cells were viable at a concentration of 50 ug/ml. Maximum inhibition was observed at 200 ug/ml conc (67%).

In conclusion, *Penicillium oxalicum* has the best effect towards synthesizing AgNPs, for antimicrobial activity against resistant bacteria and candida, in addition to anti-biofilm activity against biofilm forming *Staphylococcus aureus* and the safest cytotoxicity effect on MRC-5 cell.

REFERENCES

1. Luepke KH, Suda KJ, Boucher H, Russo RL, Bonney MW, Hunt TD, et al. Past, present, and future of antibacterial economics: increasing bacterial resistance, limited antibiotic pipeline and societal implications. *Pharmacotherapy* 2017; 37: 71-84.
2. Rai M, Kon K, Ingle A, Duran N, Galdiero S, Galdiero M. Broad-spectrum bioactivities of silver nanoparticles: the emerging trends and future prospects. *Appl*

Microbiol Biotechnol 2014; 98: 1951-1961.

3. Amini N, Amin G, Jafari Azar Z. Green synthesis of silver nanoparticles using *Avena sativa* L. extract. *Nanomed Res J* 2017; 2: 57-63.

4. Wang L, Hu C, Shao L. The antimicrobial activity of nanoparticles: present situation and prospects for the future. *Int J Nanomedicine* 2017; 12: 1227-1249.

5. Cheesbrough M (2006). District laboratory practice in tropical countries. Part 2. 2nd ed. Cambridge University Press. The Edinburgh Building, Cambridge CB2 8RU, UK.

6. The Clinical Laboratory Standards Institute (CLSI). Performance standards for antimicrobial susceptibility testing. 29th ed. CLSI supplement M100. Wayne, PA: Clinical and Laboratory Standards Institute; 2019.

7. The Clinical Laboratory Standards Institute (CLSI). Performance standards for antifungal susceptibility testing of yeast. 1st ed. CLSI supplement M60. Wayne, PA: Clinical and Laboratory Standards Institute; 2017.

8. Saeb AT, Alshammari AS, Al-Brahim H, Al-Rubeaan KA. Production of silver nanoparticles with strong and stable antimicrobial activity against highly pathogenic and multidrug resistant bacteria. *ScientificWorldJournal* 2014; 2014: 704708.

9. Ottoni CA, Simões MF, Fernandes S, Dos Santos JG, da Silva ES, de Souza RFB, et al. Screening of filamentous fungi for antimicrobial silver nanoparticles synthesis. *AMB Express* 2017; 7: 31.

10. Suriati G, Mariatti M, Azizan A. Synthesis of silver nanoparticles by chemical reduction method: effect of reducing agent and surfactant concentration. *Int J Automot Mech Eng* 2014; 10: 1920-1927.

11. Gurunathan S, Jeong JK, Han JW, Zhang XF, Park JH, Kim JH. Multidimensional effects of biologically synthesized silver nanoparticles in *Helicobacter pylori, Helicobacter felis,* and human lung (L132) and lung carcinoma A549 cells. *Nanoscale Res Lett* 2015; 10: 35.

12. Saravanan M, Vemu AK, Barik SK. Rapid biosynthesis of silver nanoparticles from *Bacillus megaterium* (NCIM 2326) and their antibacterial activity on multi drug resistant clinical pathogens. *Colloids Surf B Biointerfaces* 2011; 88: 325-331.

13. Wojnicki M, Luty-Błocho M, Kotańska M, Wytrwal M, Tokarski T, Krupa A, et al. Novel and effective synthesis protocol of AgNPs functionalized using L-cysteine as a potential drug carrier. *Naunyn Schmiedebergs Arch Pharmacol* 2018; 391: 123-130.

14. Wu Z, Tsumura Y, Blomquist G, Wang XR. 18S rRNA gene variation among common airborne fungi and development of specific oligonucleotide probes for the detection of fungal isolates. *Appl Environ Microbiol* 2003; 69: 5389-5397.

15. Hinrikson HP, Hurst SF, De Aguirre L, Morrison CJ. Molecular methods for the identification of Aspergillus species. *Med Mycol* 2005; 43 Suppl 1: S129-137.

16. Scott AC (1989). Laboratory control of antimicrobial therapy. In: *Mackie and McCartney Practical Medical Microbiology.* Eds, JG Collee, JP Duguid, AG Fraser, BP Marmion. Churchill Livingstone, 13th ed. Edinburgh, pp. 161-181.

17. Fayaz AM, Balaji K, Girilal M, Yadav R, Kalaichelvan PT, Venketesan R. Biogenic synthesis of silver nanoparticles and their synergistic effect with antibiotics: a study against Gram-positive and Gram-negative bacteria. *Nanomedicine* 2010; 6: 103-109.

18. Ishida K, Cipriano TF, Rocha GM, Weissmüller G, Gomes F, Miranda K, et al. Silver nanoparticle production by the fungus *Fusarium oxysporum*: nanoparticles characterization and analysis of antifungal activity against pathogenic yeasts. *Mem Inst Oswaldo Cruz* 2014; 109: 220-228.

19. The Clinical Laboratory Standards Institute (CLSI). Performance standards for antimicrobial susceptibility testing; twenty-second informational supplement. CLSI supplement M100-S22. Wayne, PA: Clinical and Laboratory Standards Institute; 2012.

20. Regev-Shoshani G, Ko M, Chris M, Av-Gay Y. Slow release of nitric oxide from charged catheters and its effect on biofilm formation by *Escherichia coli. Antimicrob Agents Chemother* 2010; 54: 273-279.

21. Gomha SM, Riyadh SM, Mahmmoud EA, Elaaser MM. Synthesis and anticancer activities of thiazoles, 1,3-thiazines, and thiazolidine using chitosan-grafted-poly (vinylpyridine) as basic catalyst. *Heterocycles* 2015; 91: 1227-1243.

22. Kalimuthu K, Suresh Babu R, Venkataraman D, Bilal M, Gurunathan S. Biosynthesis of silver nanocrystals by *Bacillus licheniformis. Colloids Surf B Biointerfaces* 2008; 65:150-153.

23. Kumar CM, Yugandhar P, Savithramma N. Biological synthesis of silver nanoparticles from *Adansonia digitata* L. fruit pulp extract, characterization, and its antimicrobial properties. *J Intercult Ethnopharmacol* 2016; 5: 79-85.

24. Pulcrano G, Pignanelli S, Vollaro A, Esposito M, Iula VD, Roscetto E, et al. Isolation of *Enterobacter aerogenes* carrying bla_{TEM-1} and bla_{KPC-3} genes recovered from a hospital intensive care unit. *APMIS* 2016; 124: 516-521.

25. Ansari MA, Khan HM, Khan AA, Cameotra SS, Saquib Q, Musarrat J. Gum arabic capped-silver nanoparticles inhibit biofilm formation by multi-drug resistant strains of *Pseudomonas aeruginosa. J Basic Microbiol* 2014; 54: 688-699.

26. Adebayo-Tayo BC, Popoola AO. Biogenic synthesis and antimicrobial activity of silver nanoparticle using exopolysaccharides from lactic acid bacteria. *Int J Nano Dimens* 2017; 8: 61-69.

27. Magudapathy P, Gangopadhyay P, Panigrahi BK, Nair KGM, Dhara S. Electrical transport studies of Ag nanoclusters embedded in glass matrix. *Physica B: Condensed Matter* 2001; 299: 142-146.

28. Wisam JA, Haneen AJ. A novel study of pH influence on Ag nanoparticles size with antibacterial and antifungal activity using green synthesis. *World Sci News* 2018; 97: 139-152.

29. Deljou A, Goudarzi S. Green extracellular synthesis of the silver nanoparticles using thermophilic *Bacillus* sp. AZ1 and its antimicrobial activity against several human pathogenetic bacteria. *Iran J Biotechnol* 2016;14: 25-32.

30. Nanda A, Saravanan M. Biosynthesis of silver nanoparticles from *Staphylococcus aureus* and its antimicrobial activity against MRSA and MRSE. *Nanomedicine* 2009; 5: 452-456.

31. Longhi C, Santos JP, Morey AT, Marcato PD, Durán N, Pinge-Filho P, et al. Combination of fluconazole with silver nanoparticles produced by *Fusarium oxysporum* improves antifungal effect against planktonic cells and biofilm of drug-resistant *Candida albicans. Med Mycol* 2016; 54: 428-432.

32. Jalal M, Ansari MA, Alzohairy MA, Ali SG, Khan HM, Almatroudi A, et al. Anticandidal activity of biosynthesized silver nanoparticles: effect on growth, cell morphology, and key virulence attributes of Candida species. *Int J Nanomedicine* 2019; 14: 4667-4679.

33. Masurkar SA, Chaudhari PR, Shidore VB, Kamble SP. Effect of biologically synthesized silver nanoparticles on *Staphylococcus aureus* biofilm quenching and prevention of biofilm formation. *IET Nanobiotechnol*

34. Gupta K, Barua S, Hazarika SN, Manhar AK, Nath D, Karak N, et al. Green silver nanoparticles: enhanced antimicrobial and antibiofilm activity with effects on DNA replication and cell cytotoxicity. *RSC Adv* 2014; 4: 52845-52855.

35. Kalishwaralal K, BarathManiKanth S, Pandian SR, Deepak V, Gurunathan S. Silver nanoparticles impede the biofilm formation by *Pseudomonas aeruginosa* and *Staphylococcus epidermidis. Colloids Surf B Biointerfaces* 2010; 79: 340-344.

36. Chávez-Andrade GM, Tanomaru-Filho M, Basso Bernardi MI, de Toledo Leonardo R, Faria G, Guerreiro-Tanomaru JM. Antimicrobial and biofilm anti-adhesion activities of silver nanoparticles and farnesol against endodontic microorganisms for possible application in root canal treatment. *Arch Oral Biol* 2019; 107: 104481.

37. Mahmoudi M, Laurent S, Shokrgozar MA, Hosseinkhani M. Toxicity evaluations of superparamagnetic iron oxide nanoparticles: cell "vision" versus physicochemical properties of nanoparticles. *ACS Nano* 2011; 5: 7263-7276.

38. Fabrega J, Renshaw JC, Lead JR. Interactions of silver nanoparticles with *Pseudomonas putida* biofilms. *Environ Sci Technol* 2009; 43: 9004-9009.

39. Yen HJ, Hsu SH, Tsai CL. Cytotoxicity and immunological response of gold and silver nanoparticles of different sizes. *Small* 2009; 5: 1553-1561.

40. Moteriya P, Chanda S. Biosynthesis of silver nanoparticles formation from *Caesalpinia pulcherrima* stem metabolites and their broad spectrum biological activities. *J Genet Eng Biotechnol* 2018; 16:105-113.